https://doi.org/10.5194/egusphere-2026-4880
Preprint. Discussion started: 18 August 2026

High centennial-scale variability in an East Antarctic snow accumulation record spanning the last millennium

Max T. Nilssen[1,2], Tessa R. Vance[3,4], Poul Christoffersen[1,2], Sue Cook[4], Alison S. Criscitiello[5], and Nerilie J. Abram[3]

[1]Institute for Marine & Antarctic Studies, University of Tasmania, Battery Point, TAS 7004, Australia
[2]Australian Centre for Excellence in Antarctic Science, Institute for Marine & Antarctic Studies, University of Tasmania, Battery Point, TAS 7004, Australia
[3]Australian Antarctic Division, Department of Climate Change, Energy, the Environment and Water, Kingston, TAS 7050, Australia
[4]Australian Antarctic Program Partnership, Institute for Marine and Antarctic Studies, University of Tasmania, Battery Point, TAS 7004, Australia
[5]Department of Earth & Atmospheric Sciences, University of Alberta, Edmonton, Alberta, Canada

Correspondence: Max Nilssen (max.nilssen@utas.edu.au)

Abstract. Mass balance estimates of the East Antarctic ice sheet over the satellite era have a high degree of uncertainty, yet are of such significance that they can partially or even entirely offset the ice loss at the margins of the Antarctic Ice Sheet that contributes to global sea level rise. Therefore, it is imperative to improve our understanding of snowfall variability across time and space in East Antarctica. Here we present a new millennial-scale, annual snow accumulation history from the Mount Brown South (MBS) ice core, a semi-coastal record from 2,084 m elevation on the boundary of Wilhelm II and Princess Elizabeth Land in East Antarctica. We used a range of methods to test the best derivation of annual accumulation rates, and to ensure best practice in determining both density correction and layer thinning with depth. The MBS annual accumulation record spans 873-2017 CE, and displays a high degree of variability across time scales. The long-term mean snow accumulation rate at MBS is 0.276 ± 0.08 (1 standard deviation) $\mathrm{m\,yr^{-1}}$ ice equivalent, which is almost 10% lower than the mean accumulation rate in the satellite era (1979-2017) of 0.302 ± 0.08 $\mathrm{m\,yr^{-1}}$ ice equivalent. While mean annual accumulation during the satellite era is within the range of natural variability, the full record exhibits substantial decadal to centennial-scale variability, including two notable low accumulation periods between CE 1127–1321 (195 years) and 1754–1879 (126 years), where accumulation was 12% lower than the long-term mean, and 20% lower than satellite era mean. While an ice core record is a point-based rather than spatially resolved estimate of annual accumulation, these results raise implications for future mass balance assessments in this region that assume the satellite era represents the natural range of variability.

1 Introduction

The East Antarctic Ice Sheet (EAIS) is the largest reservoir of freshwater on Earth, so understanding the rate and variability of snow accumulation under changing climatic conditions is crucial. With a paucity of records to constrain snowfall, there is significant uncertainty in East Antarctic contributions to sea level change. Recent estimates of EAIS mass balance show

https://doi.org/10.5194/egusphere-2026-4880
Preprint. Discussion started: 18 August 2026

large disagreements between methods and it remains unclear whether the EAIS is gaining or losing mass (Stokes et al., 2022; Otosaka et al., 2023). Several studies report an increase in EAIS mass due to increased rates of snowfall over the last few decades (e.g. Shepherd et al., 2018; Bamber et al., 2018), however other studies report a mass loss (Shepherd et al., 2019; Rignot et al., 2019; Schröder et al., 2019). Exceptionally high snowfall across Antarctica in 2022, likely driven by an increased frequency of atmospheric river events, resulted in a temporary gain in ice sheet mass, and a pause in Antarctica's contribution to global sea level rise (Wang et al., 2023; Wille et al., 2024). Surface mass balance, which is dominated by snowfall variability, represents the largest source of uncertainty in EAIS mass balance estimates (Stokes et al., 2022). It is therefore critical to constrain uncertainties in snowfall estimates.

Ice core records extend the climate record and contextualize recent trends and extremes in precipitation variability on annual to multi-centennial timescales. However, millennial-scale, annually resolved ice core records are scarce in the Indo-Pacific sector of East Antarctica (Vance et al., 2024, 2016; Thomas et al., 2017, 2023). Only one other existing ice core record from this region (Law Dome, Dome Summit South (DSS)) spans the past two millennia at annual resolution (Roberts et al., 2015; Jong et al., 2022). The Mount Brown South (MBS) location was chosen to provide a new, complementary understanding of past variability in the Indo-Pacific sector, with site selection parameters that deliberately emphasized atmospheric moisture source regions that were distinct from those of Law Dome in order to ensure a new, independent assessment of point-based snowfall accumulation could be made (Vance et al., 2016).

Ice core studies commonly investigate whether signals of modes of variability are preserved in physico-chemical features of the record, with the Southern Annular Mode (SAM) (Marshall, 2003) and El Niño-Southern Oscillation (ENSO) (McPhaden et al., 2006) being the principle modes investigated in Antarctica (Medley and Thomas, 2019; Udy et al., 2026; Vance et al., 2013, 2022). Crockart et al. (2021) investigated satellite era annual snow accumulation at MBS (prior to the derivation of the full record presented here) and found no relationship with the SAM. Over the satellite era, Udy et al. (2026) hypothesize that synoptic-scale weather variability masks the SAM signal in the MBS ice core record, because SAM–like synoptic patterns only constitute a small percentage of the weather systems delivering snowfall to MBS (Udy et al., 2021, 2026). Understanding how representative this analysis is over longer timescales is a difficult but critical goal (Jones et al., 2016).

At ice core sites with sufficiently high mean annual snowfall (e.g. DSS and MBS) annual cycles can be discerned in both stable water isotope ratios and trace chemistry concentrations, to develop annually resolved age-at-depth models (chronologies). Aligning specific non-sea-salt sulphate peaks to known volcanic horizons provides an additional chronological verification (e.g. Winstrup et al. (2019); Vance et al. (2024)). However, the observed thickness of the annual layers must be corrected for variations in density with depth due to firn densification (Herron and Langway, 1980), and for layer thinning due to ice flow (Nye, 1963). In this study, we present the annual snow accumulation history at MBS for 873-2017 CE after accounting for these glacio-dynamic factors using a range of approaches, and following the published MBS chronology (Vance et al., 2024). This study provides a foundational new baseline record with which to investigate past variability in snowfall rates, extreme precipitation events, and multi-decadal to centennial changes in surface mass balance for this region.

https://doi.org/10.5194/egusphere-2026-4880
Preprint. Discussion started: 18 August 2026

2 Data

2.1 Mount Brown South site description

The MBS site (69.111°S, 86.312°E, 2,084 m asl) is 340 km to the east of Davis station, 240 km inland from the West Ice Shelf, and 1140 km west of the Law Dome, DSS ice core site. The ice thickness is approximately 2000 m (Vance et al., 2016). The prevailing wind direction in the MBS region is ESE, with higher precipitation associated with winds directly from the east, and lower snowfall when the winds are more southeasterly (Vance et al., 2024). Previous studies found that snowfall accumulation at MBS follows a seasonal cycle, with higher precipitation in the austral polar winter (March-October), and lower precipitation during December-January, but high precipitation events can occur in any month (Crockart et al., 2021; Jackson et al., 2023).

Four ice cores were drilled at MBS in 2017/2018: a 295 m intermediate length core (MBS-Main), and three 20-25 m surface cores (MBS-Alpha, MBS-Bravo, MBS-Charlie) (Crockart et al., 2021; Vance et al., 2024; Gkinis et al., 2024). Site selection emphasised minimal melt and surface reworking, sub-annual resolution (using standard ice core analytical techniques) and reduced horizontal ice advection through time. An atmospheric link to mid-latitude circulation in the Indian Ocean which was independent to that of Law Dome was also desirable (Vance et al., 2016). Details of drilling, ice core processing, chemical analysis, and chronology development can be found in Crockart et al. (2021), Jackson et al. (2023), Gkinis et al. (2024), Harlan et al. (2025, 2026) and Vance et al. (2024).

Here, we use the unconstrained annual layer thicknesses from the MBS-Main (CE 873-1989) and the MBS-Charlie (CE 1990–2017) ice core chronologies (Vance et al., 2024). The 1989/1990 annual horizon that is used to splice the Main (deep) and Charlie (surface) cores was characterized by a very prominent water isotope peak which was clearly aligned across the MBS-Main and surface cores, and is book-ended by clear minima in sea salt concentrations. In addition, 1990 is not within 10 years of the bottom or top of any individual record, and is furthermore close to the clear non-sea-salt sulphate eruption signal of Pinatubo (Philippines, mid-1991) in all site cores.

2.2 Density measurements

Length, diameter and weight were recorded during field processing of each ∼1 m length of ice core from MBS-Main (Hans Tausen drill), from 4 m to 294.6 m depth. Diameter measurements were averaged from two-three measurements for each core section for the top 96 m (above to the approximate transition to glacial ice). From 97 m depth, the diameter stabilized at 98.1 mm, and no further diameters were measured. Mass was measured in kg up to 3 significant figures, and the bulk density of each core was estimated using:

$$\rho = \frac{m}{\pi r^2 l} \quad (1)$$

where ρ is the mean density of a core section, m is mass in kg, r is radius (diameter/2) and l is length.

For this study, the MBS-Main core density measurements were quality controlled, and poor estimates of density resulting from missing ice core material, e.g. from drilling "dog drags" or core breaks were not included in density modelling (see Sect. 3.1). This assessment was subjective but considered, in order to get the best representation of downcore density change.

https://doi.org/10.5194/egusphere-2026-4880
Preprint. Discussion started: 18 August 2026

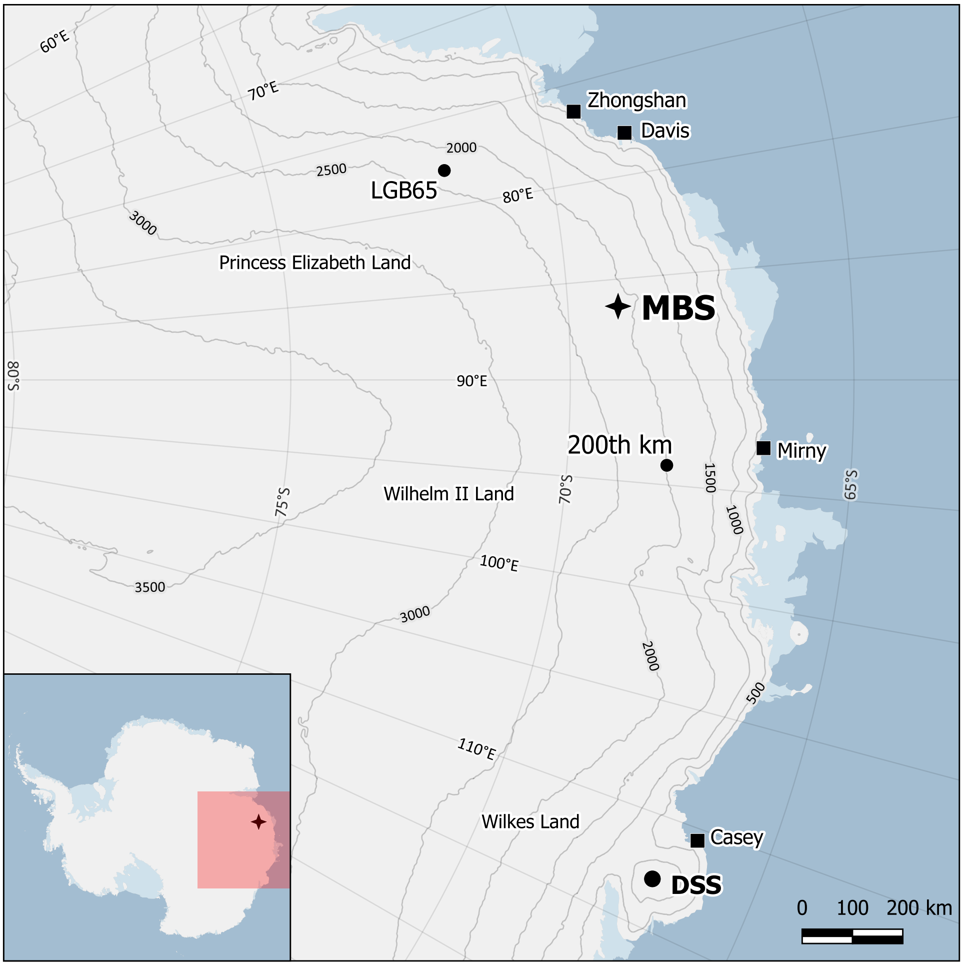

Figure 1. MBS drill site (star) and other regionally co-located ice core sites with annually resolved accumulation records spanning > 250 years (circles, see Table S1). Antarctic stations (Zhongshan (China), Davis (Australia), Mirny (Russia) and Casey (Australia)) are shown (squares). Contours show 500 m surface elevations (Helm et al., 2014). Map made using Quantarctica for QGIS (Matsuoka et al., 2021).

https://doi.org/10.5194/egusphere-2026-4880
Preprint. Discussion started: 18 August 2026

No density measurements were made of the surface cores, thus the first density measurements were at 4 m. We use density measurements from a surface core drilled in the MBS region (69.131°S, 85.999°E, 2078 m elevation, 12.65 km from the 2017/2018 MBS drill site) in December 1998 to validate the top 10 m of the density-depth relationship derived from the MBS-Main density measurements (see Section 3.1, Fig. 2). See Smith and Ruddell (2001) and Smith et al. (2002) for details of this earlier study.

2.3 ApRES vertical displacement data

An ApRES (autonomous phase-sensitive radio-echo sounder) instrument collected data at the MBS site from 9th Dec 2017 to 21st Jan 2018. ApRES data provide distance to internal reflectors in the ice, which can be used to calculate vertical strain rates. The instrument emitted a burst of 50 chirps every 90 minutes. This time series data was processed using the method established by Vaňková et al. (2020). We averaged all the chirps from each burst to improve the signal-to-noise ratio, creating a timeseries of phase and amplitude vs. depth. The depth profile was then divided into 5 m segments, and we created a timeseries of vertical displacement for each segment. This was done by cross-correlating each consecutive pair of measurements. The first ten days of data were discarded due to disturbance during the installation of the equipment, which caused high levels of noise in the vertical displacement. The data from 24th December 2017 were also removed because it had anomalously low displacement across all vertical layers, most likely because of some disturbance at the surface. The ApRES vertical displacement data were used to calculate the uniform vertical strain rate at the MBS site (see Sect. 3.2)

3 Methods

3.1 Density-depth relationship

We developed an empirical density-depth relationship for MBS using the same form as the empirical relationship derived for Law Dome, first presented in Van Ommen et al. (1999). The quality-controlled core density measurements were used to derive the parameters in Eq. 2:

$$\rho(d) = \rho_{\mathrm{ice}} - c_{\mathrm{f}} \exp\left(\frac{-d}{k_{\mathrm{f}}}\right) + \begin{cases} c_0 + rd & \text{if } d < d_b \\ -c_{\mathrm{s}} \exp\left(\frac{-d}{k_{\mathrm{s}}}\right) & \text{if } d \geq d_b \end{cases} \quad (2)$$

where d is depth below the surface in metres, ρ is density, $\rho_{\mathrm{ice}} = 917\ \mathrm{kg\,m^{-3}}$, $c_{\mathrm{f}} = 118.88\ \mathrm{kg\,m^{-3}}$, $k_{\mathrm{f}} = 8.2274$ m, $c_0 = -359.56\ \mathrm{kg\,m^{-3}}$, $r = 3.7690\ \mathrm{kg\,m^{-4}}$, $d_{\mathrm{b}} = 62.944$ m, $c_{\mathrm{s}} = 850.68\ \mathrm{kg\,m^{-3}}$, $k_{\mathrm{s}} = 32.457$ m. All parameters take their best-fit values determined using non-linear least squares, except for k_{s}, which was calculated for continuity at d_{b}. In the upper part of the firn column, the relationship is described by the combination of a linear trend with an exponential. Below the parameterized "break" depth, the linear component is replaced with another exponential term, to allow the equation to approach the density of glacier ice. To make the conversion to ice equivalent, the observed layer thickness from the chronology was multiplied by the modelled density at the mid-point depth of the annual layer, then divided by the density of glacier ice ($917\ \mathrm{kg\,m^{-3}}$).

https://doi.org/10.5194/egusphere-2026-4880
Preprint. Discussion started: 18 August 2026

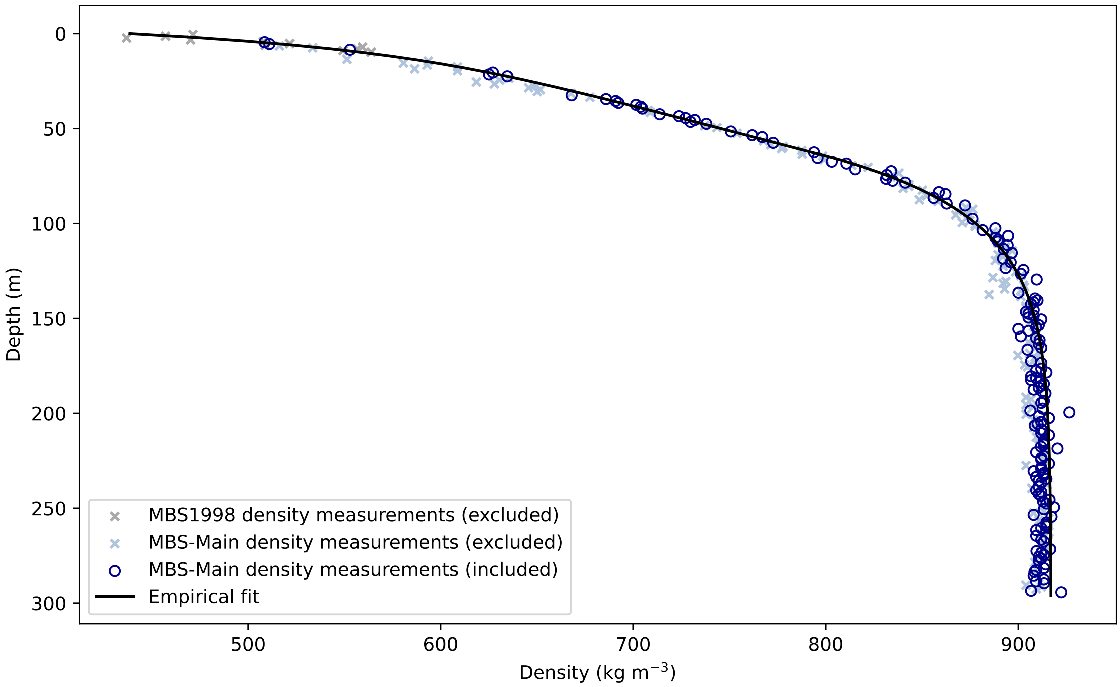

Figure 2. MBS density profile, showing the quality controlled density measurements from MBS-Main (open dark blue circles), density measurements from MBS-Main not included in density fit (light blue crosses), density measurements from MBS1998 (grey crosses, not included in density fit), and empirically derived fit calculated using Eq. 2 (black line). There is good agreement between the empirical fit and the density measurements.

3.2 Strain thinning adjustment

115 The observed thickness of a given ice layer is dependent on its vertical strain rate history - i.e., how much it has thinned vertically and stretched horizontally due to deformation. A "thinning function" can be derived to relate the observed layer thickness to its initial thickness, i.e. the original accumulation rate:

$$\lambda = F\,\dot{b} \tag{3}$$

Where λ is the observed layer thickness in ice equivalent, F is the thinning function, and $\dot{b}$ is the accumulation rate. F can
120 be a function of either depth or age, and is equal to 1 at the surface (nil strain thinning) and decreases with depth. The vertical strain rate can be estimated using ice flow models (e.g. Nye, 1963; Dansgaard and Johnsen, 1969), or by fitting measurements of ice velocity to linear or non linear models (e.g. Roberts et al., 2015; Winstrup et al., 2019). Dansgaard and Johnsen (1969)

https://doi.org/10.5194/egusphere-2026-4880
Preprint. Discussion started: 18 August 2026

developed a model that assumes the vertical strain rate takes a constant value from the surface down to some height above the bed, then decreases linearly to zero at the base. For a typical horizontal velocity profile in an ice sheet, the constant vertical strain rate section covers the top 50% to 80% of the ice sheet height (Cuffey and Paterson, 2010, p. 619). The MBS ice core spans approximately the upper 15% of the ice sheet, thus we assume a constant vertical strain rate. We compared two different strain thinning adjustment methods – using theory (Nye (1963)) and observations (ApRES), both of which assume a uniform vertical strain rate. See Sect. S1 for a description of the implementation for the Nye model for MBS.

Here we used vertical displacement data from the ApRES measurements to calculate a uniform vertical strain rate. After processing the ApRES vertical displacement data, we calculated a linear fit to the vertical displacement over time, to give an average rate of displacement for each layer. The vertical strain rate is given by the gradient of the rate of vertical displacement over depth. If the strain rate is depth-independent, the slope will be linear. We excluded the top 120 m from the fit, because this section is affected by firn densification. The layers 120-292 m were also excluded, because the radar return over this depth range was affected by interference from the nearby drilling process (removed data points are shown as magenta in Fig. S2). Thus the layers from 293-800 m were used for the linear fit. The linear vertical fit produced a vertical strain rate of $-2.59 \times 10^{-4} \pm 1.5 \times 10^{-5}$ year^{-1} (the strain rate is negative, indicating compression), calculated using Matlab's linear regression model. We then used the vertical strain rate to adjust for strain thinning using this equation from Cuffey and Paterson (2010):

$$\dot{b}(a) = \lambda(a)\exp(-\dot{\epsilon}_z a) \tag{4}$$

Where $\dot{b}$ is annual accumulation rate, a is years before drilling, λ is observed layer thickness in ice equivalent, and $\dot{\epsilon}_z$ is the vertical strain rate. Thus the thinning function is $\exp(\dot{\epsilon}_z a)$.

To construct the MBS snowfall accumulation record, we used the ApRES derived vertical strain rate (rather than the Nye model). We preferred the ApRES method because it uses observational data, and does not rely on the assumptions made by the Nye model. We did however compare our preferred strain thinning adjustment method (ApRES) with the long-term accumulation calculated using the Nye model (Fig. S1 and Sect.5.4). The Nye method results in a mean accumulation rate of 0.256 ± 0.08 m yr^{-1} ice equivalent, and the record exhibits a positive trend. In contrast, the ApRES approach did not result in any significant trend in annual accumulation through time. Our discussion thus focuses on the ApRES-derived result.

3.3 Regime shift analysis

We carried out regime shift analysis using the STARS (Sequential t-test Analysis of Regime Shift) method (Rodionov, 2004). This method has been used to detect regime shifts in various systems, including climatic and atmospheric sciences (Jaagus et al., 2017). We used the Rodionov function from the rshift library in R (Rodionov, 2004; Room et al., 2025) to detect regime shifts in annual snowfall accumulation at MBS. This function steps along the dataset, and tests whether each value in the current regime deviates significantly from the regime average. If a deviation is detected, the algorithm tests if the shift is persistent. A regime shift index (RSI) is used to quantify the magnitude of the shift, and the algorithm restarts, using the shift point as

https://doi.org/10.5194/egusphere-2026-4880
Preprint. Discussion started: 18 August 2026

the beginning of a new regime. The Rodionov function takes a parameter l, which is essentially the predicted length for each regime. We used $l = 50$ to detect regimes on the multidecadal to centennial scale. We ran the algorithm chronologically, i.e. from the oldest layer to the newest layer, and used the significance cut off p=0.05. We disregarded the regime shifts that were detected in the final cut off window (i.e. within 50 years of 2017 CE), as the STARS method may return false regime shifts towards the end of the time series (Stirnimann et al., 2019).

3.4 Comparison to the Southern Annular Mode and selected Antarctic ice core accumulation records

We calculated Pearson correlations (after calculating effective degrees of freedom according to Bretherton et al. (1999)) between the MBS annual accumulation history, regionally adjacent (within $\sim$ 1200 km of MBS) Antarctic ice core accumulation histories spanning multiple centuries (see Table S1) and annual SAM indices and reconstructions (Abram et al., 2014; Dätwyler et al., 2018; King et al., 2023; Fogt et al., 2009; Marshall, 2003). We also computed correlations after Gaussian smoothing the time series to the equivalent of 3-15 year running mean (sigma = 1.5, 3, 5).

4 Results

4.1 Long term variability in accumulation at Mount Brown South

When corrected for densification using our empirical densification model and strain thinning using ApRES vertical displacement measurements, the long term mean annual accumulation rate at MBS (873-2017) is 0.276 $\pm$ 0.08 (1 standard deviation) $\mathrm{m\ yr^{-1}}$ ice equivalent (Fig. 3). Regime shift analysis identified nine distinct accumulation regimes (from 48–254 years long) across the full MBS period, where the accumulation rates diverge from the long term mean (Figs. 3, 4 and Table 1). The period with the lowest annual accumulation is a relatively short period (1461-1508, mean annual accumulation = 0.232 $\mathrm{m\ yr^{-1}}$ ice equivalent) which was 15.7% below the long term mean. This period followed a high accumulation regime lasting more than a century (1322-1460, mean annual accumulation = 0.298 m $\mathrm{yr^{-1}}$ ice equivalent). The change point in 1461 is the most significant in the study period (indicated by the highest regime shift index, see Table S2), and results in a significant and sudden negative trend in the mid-late 15th century. The regime with the highest mean annual accumulation is 1595-1650 (mean accumulation = 0.317 $\mathrm{m\ yr^{-1}}$ ice equivalent, 15.0 % higher than long term mean), and is preceded and followed by two near-mean regimes. Probability density functions (PDFs) of the high accumulation regimes exhibit a skew to the upper tail of the distribution compared to the long term distribution, indicating an increased frequency in unusually high accumulation years (Fig. 4). The PDFs of the low accumulation regimes show a skewness toward the lower tail of the distributions. This indicates that accumulation regimes that differ significantly from the long-term distribution are driven by a tendency toward greater numbers of anomalously low or high accumulation years, rather than a general increase or decrease in accumulation in all years.

https://doi.org/10.5194/egusphere-2026-4880
Preprint. Discussion started: 18 August 2026

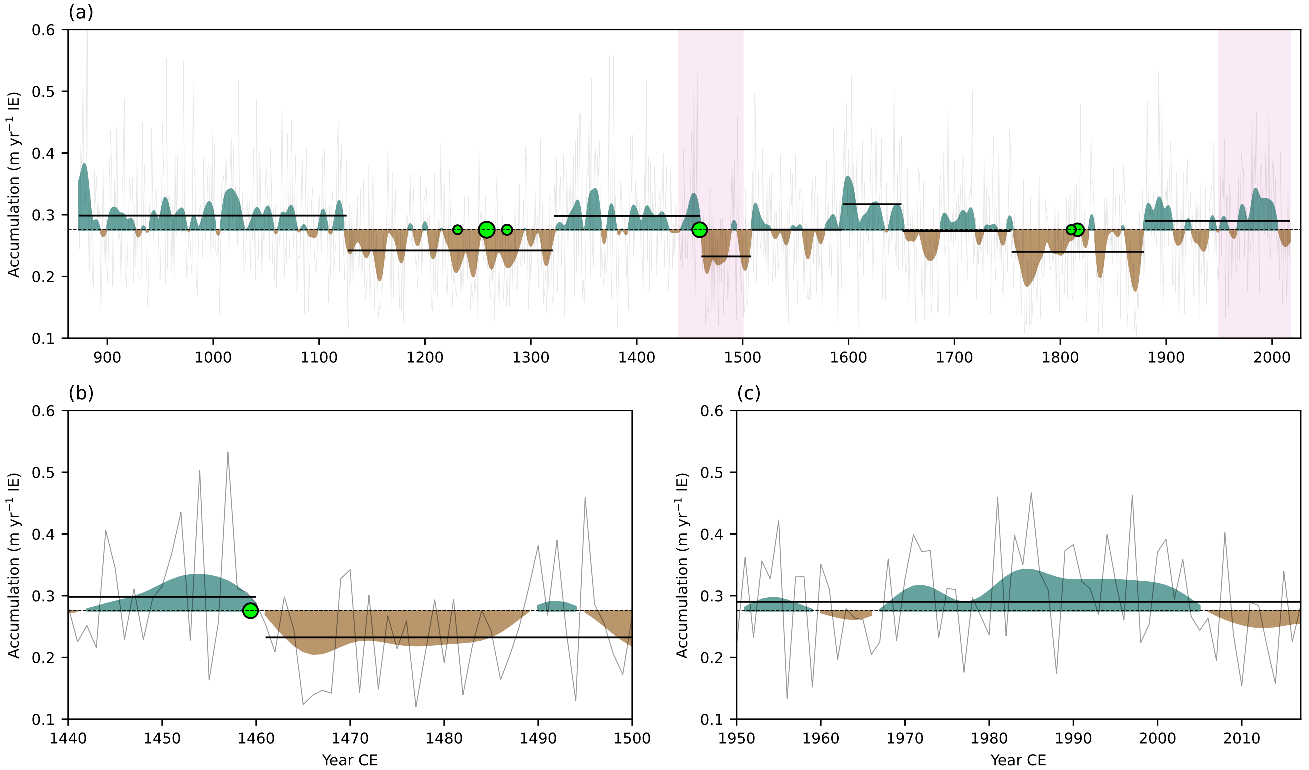

Figure 3. The MBS accumulation rate history for (a) the full length of the MBS ice core (873-2017) and two periods of specific variability: (a) 1440-1500 and (b) 1950-2017 (shown with pink shading in panel (a)). The annual accumulation (grey lines) is overlayed with the long term mean (0.276 m yr^{-1} ice equivalent (IE), dashed horizontal), and is then Gaussian smoothed (sigma=3, roughly equal to a 10-year running mean) (brown = below long-term mean, teal = above long-term mean). Also shown are mean accumulation rates between regime shift points (see Table 1, black bars). The six largest volcanic sulfate deposition events in the last millennium (1230, 1258, 1277, 1459, 1810, 1816) are shown with green circles (Sigl et al., 2014)). The date of the circles is that identified in the MBS chronology (Vance et al., 2024), and the size of the circles corresponds to the average sulfate deposition from a compilation of Antarctic ice core records (Sigl et al., 2014).

https://doi.org/10.5194/egusphere-2026-4880
Preprint. Discussion started: 18 August 2026

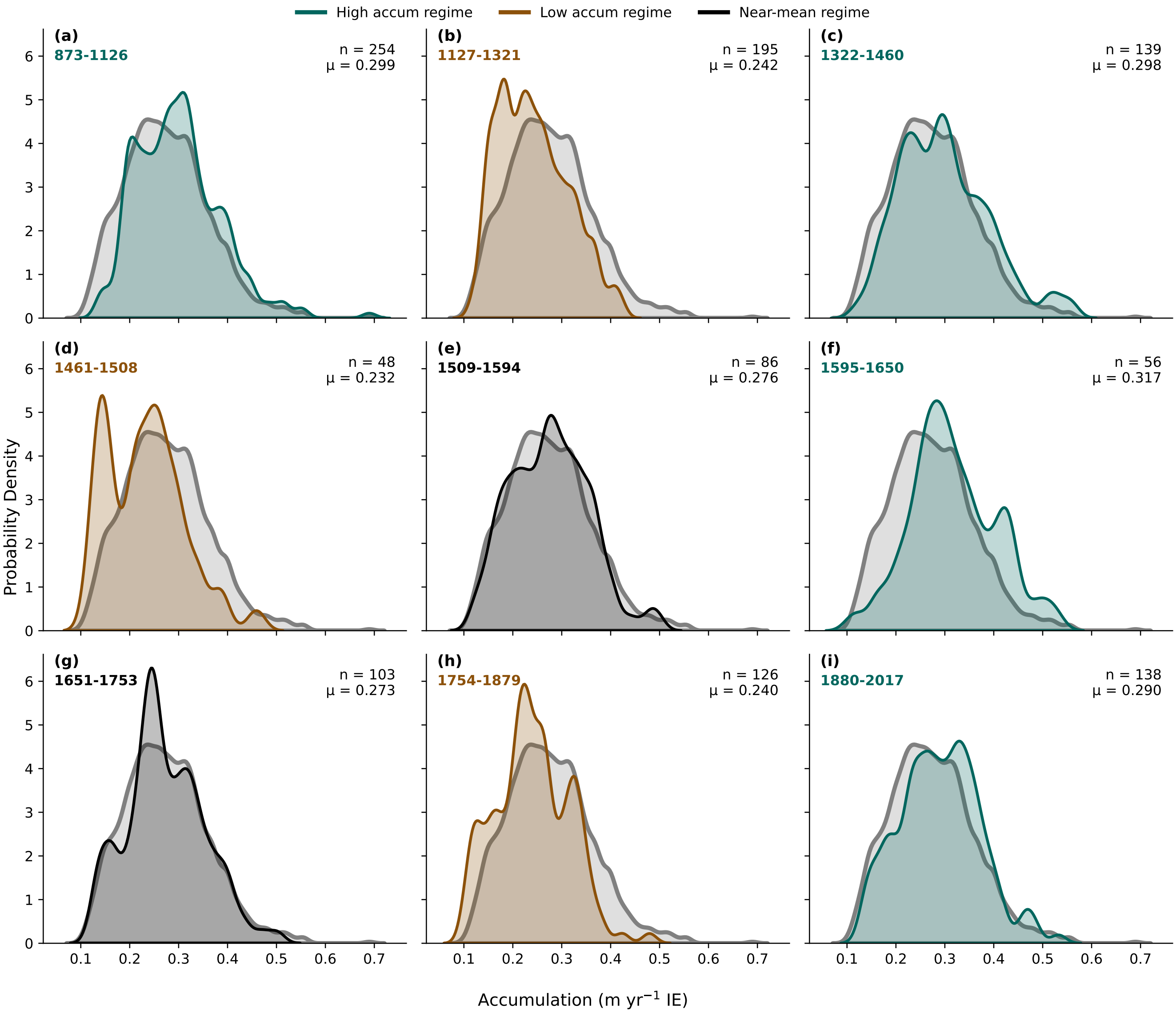

Figure 4. Probability density functions (PDFs) of annual accumulation rates for the nine accumulation regimes identified with regime shift analysis. In each panel, the coloured curve represents the PDF of accumulation rates for the regime indicated in the panel label, while the grey curve shows the PDF for the full MBS ice core period (873-2017), for comparison. The number of years in each regime (n) and the mean accumulation of the regime (μ) are shown for each regime. Regimes are classified according to their mean accumulation relative to the long term mean (teal = high accumulation regime, brown = low accumulation regime, black = near-mean regime). PDFs were calculated using a Gaussian kernel with a bandwidth adjustment factor of 0.5. Differences in the location, spread and shape of the regime distributions relative to the full record distribution highlight periods of sustained departures from the long-term mean.

https://doi.org/10.5194/egusphere-2026-4880
Preprint. Discussion started: 18 August 2026

Table 1. Characteristics of accumulation regimes identified by regime shift analysis.

Regime (CE)	Duration (yr)	Mean ± SD (m yr^{-1} ice equivalent)	% Difference from Long-term Mean
873–1126	254	0.299 ± 0.085	8.3
1127–1321	195	0.242 ± 0.071	-12.2
1322–1460	139	0.298 ± 0.092	8.2
1461–1508	48	0.232 ± 0.079	-15.7
1509–1594	86	0.276 ± 0.080	0.1
1595–1650	56	0.317 ± 0.087	15.0
1651–1753	103	0.273 ± 0.079	-0.8
1754–1879	126	0.240 ± 0.075	-12.9
1880–2017	138	0.290 ± 0.082	5.3

4.2 Independence of the MBS snow accumulation record

After accounting for autocorrelation, we found no significant correlations between MBS annual snow accumulation and any of the most commonly used SAM reconstructions or indices over all time periods of interest (e.g. 1979–2017, 1957–2017, CE 873–2017) (Abram et al., 2014; Dätwyler et al., 2018; King et al., 2023; Fogt et al., 2009; Marshall, 2003). We also found no clear evidence to suggest snowfall variability at MBS is directly attributable to volcanic eruptions, since only one of the eight accumulation regime shifts coincides with a known volcanic event, i.e. Kuwae (Vanuatu) in 1459 (Fig. 3b). In addition, we found no significant correlation between MBS annual accumulation and the three closest sites (located 328-1127 km from MBS) where annual accumulation has been previously published (see Table S1 for details and Fig. 1 for locations).

5 Discussion

5.1 Long term variability in Mount Brown South snow accumulation and comparison to Law Dome

The MBS annual snowfall accumulation record is a new millennial-length record spanning CE 873-2017 (1,145 years). MBS exhibits a high degree of snowfall accumulation variability at interannual, decadal and centennial scales, with sustained multi-decadal and centennial length periods of accumulation that diverge from the long term mean. We have shown that the accumulation variability is unrelated to variability in the SAM, and is uncorrelated with other annual accumulation records from ice cores in the Indian Ocean sector of East Antarctica. Of particular note, MBS displays centennial scale variability in accumulation that is not present in the Law Dome DSS 2,000 year annual accumulation record (Fig. 5), (Roberts et al., 2015; Jong et al., 2022). Accumulation at Law Dome is highly variable on the interannual scale, with pronounced decadal variability, whereas MBS also shows clear centennial-scale variability. This difference is important because the Law Dome record is the longest annually resolved accumulation record in the Wilkes Land region of East Antarctica. With no other millennial length records available, studies of snowfall and surface mass balance in this sector of East Antarctica have so far been heavily influenced

https://doi.org/10.5194/egusphere-2026-4880
Preprint. Discussion started: 18 August 2026

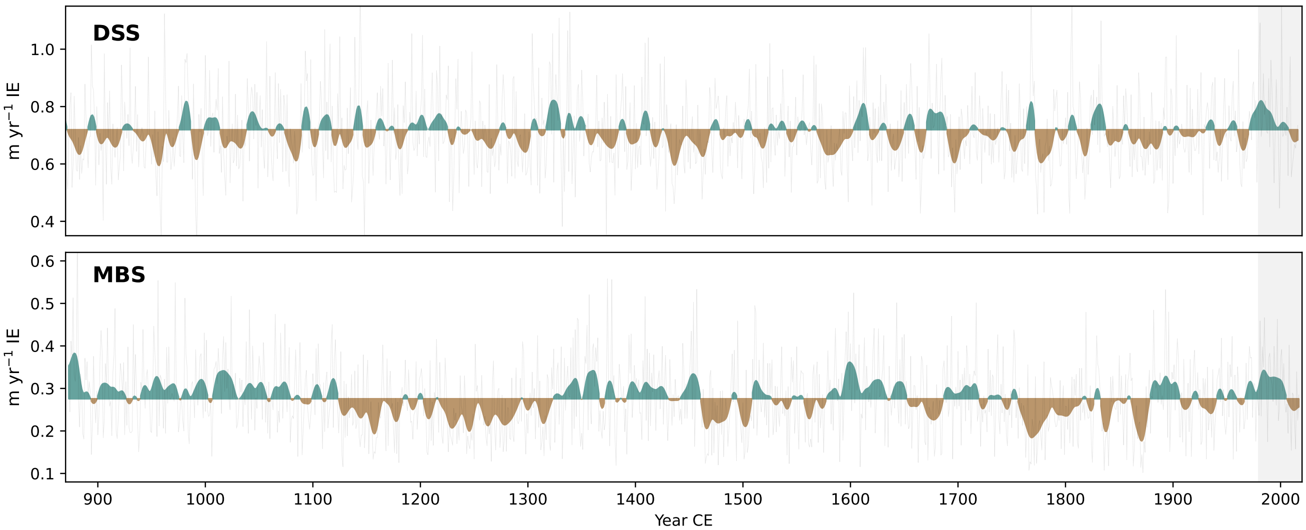

Figure 5. Annual snow accumulation rate for MBS (bottom panel) and DSS (top panel), with Gaussian smoothed accumulation rates (sigma=3, roughly 10 year running mean). Colour shading represents periods of accumulation above (teal) or below (brown) the respective long term mean. MBS and DSS display contrasting temporal variability, with centennial-scale variability at MBS that is not seen at DSS. The satellite era is shaded in grey. Note the y axes are on different scales.

by the Law Dome accumulation record (e.g. Thomas et al., 2017; Frezzotti et al., 2013). The new MBS accumulation record developed here shows that snowfall in East Antarctica is significantly more spatially variable than expected, and may be far more temporally variable than would otherwise be assumed from studying the Law Dome record alone.

Perhaps the most striking aspect of the centennial-scale variability in the new MBS record is the low accumulation regime in the 12th and 13th centuries. This regime (1127–1321 CE) had a mean accumulation rate of 0.242 $\mathrm{m\,yr^{-1}}$ ice equivalent, 12 % lower than the long term mean and 22 % lower than the satellite era mean. While the Law Dome annual accumulation record exhibits far less temporal variability in snow accumulation, the Law Dome summer sea salt record (December–March mean sodium or chloride concentrations) does display centennial-scale variability, including a lower than average period in the 12th and into the 13th centuries (Vance et al., 2013). The Law Dome summer sea salt record has been linked to both ENSO and eastern Australian rainfall variability, and used to infer a multi-decade megadrought during the 12th century in eastern Australia (Vance et al., 2013, 2015), related to variability in relative phasing of the Interdecadal Pacific Oscillation (Vance et al., 2022). Analysis of the distribution (PDFs) of the 1127–1321 regime shows a bimodal distribution, with two peaks of low accumulation years centred around 0.2 $\mathrm{m\,yr^{-1}}$ ice equivalent (Fig. 4b). This regime is dominated by low accumulation years, with a distinct lack of high accumulation years. As discussed in Sect. 5.3, accumulation variability at MBS is driven by high precipitation events, associated with meridional moisture transport from synoptic-scale weather systems in the southern Indian Ocean (Jackson et al., 2023; Udy et al., 2026). We suggest that in low accumulation regimes, circulation in the southern Indian

Ocean tended less towards the synoptic conditions that lead to meridional moisture flux, leading to years where, by chance, fewer of the synoptic set-ups that lead to high or extreme snowfall events at the MBS site occur.

5.2 Accumulation regime shifts at Mount Brown South

The MBS accumulation record exhibits multiple, relatively rapid, shifts from one regime type to another. Two particular decadal to centennial regime shifts stand out. Between 1322 and 1460, mean accumulation was 0.298 $\mathrm{m\,yr^{-1}}$, similar to the satellite era. A sharp shift in 1461 marks the beginning of a 48 year period of significantly lower mean annual accumulation of 0.232 $\mathrm{m\,yr^{-1}}$ (CE 1461–1508). This 22 % reduction results in a significant and sudden negative trend in accumulation rate at MBS in the mid 15th century (Fig. 3b). The second transition is more recent. Between 1754 and 1876, the mean accumulation rate was low, at 0.239 $\mathrm{m\,yr^{-1}}$. The shift at 1877 to a higher accumulation regime (0.290 $\mathrm{m\,yr^{-1}}$ between 1877–2017) is equivalent to a 21% increase and results in a significant positive trend in the mid-late 19th century. The later part of the 1877–2017 regime overlaps with observational data for this region, and indeed most of the Southern Hemisphere. While the shift in 1461 coincides with the large Kuwae eruption of 1459, it is difficult to perceive any obvious relationship between the sustained MBS accumulation regimes and large volcanic eruptions, as this shift is the only time a large eruption and an accumulation regime shift coincides, and it is not clear how short-term forcing of a volcanic event could result in a half-century of sustained low accumulation. This does not preclude an influence of the Kuwae eruption on SH mid-latitude circulation, which would obviously influence the accumulation regime at MBS, however our results clearly show accumulation shifts at MBS on the centennial scale to be generally unrelated to large eruptions.

5.3 Satellite era context

Our results extend and contextualise a previous satellite era study of annual snowfall accumulation at the MBS site, which found that mean annual satellite era accumulation at MBS was between 0.295 and 0.309 $\mathrm{m\,yr^{-1}}$ ice equivalent (for the MBS-Alpha, MBS-Charlie and MBS-Main cores) (Crockart et al., 2021). This is comparable to the satellite era value we found of 0.302 $\pm$ 0.08 $\mathrm{m\,yr^{-1}}$ ice equivalent (1979-2017). The mean accumulation during the satellite era is about 10% higher (0.33 standard deviations) than the mean during the prior 11 centuries (873-1978, mean = 0.275 $\mathrm{m\,yr^{-1}}$ ice equivalent). This indicates that recent accumulation is within the range of long term natural variability and is not exceptionally high relative to the last millennium. We find a negative trend in MBS accumulation rate over the satellite era, equal to -0.026 m ice equivalent per decade (p=0.02) (see Fig. 3c). The Law Dome accumulation record also exhibits a similar negative trend. This aligns with recent studies that show the glacier drainage basins containing MBS and Law Dome have experienced a negative trend in total precipitation owing to a negative trend in the frequency of atmospheric rivers in this region (Wille et al., 2025; Maclennan et al., 2022). This has implications for estimations of surface mass balance and mass balance, and therefore estimations of sea level change. The basin-integrated surface mass balance (from an ensemble of nine models) for the drainage basin containing MBS was found to be 163 $\mathrm{Gt\,yr^{-1}}$ over 1980-2010 (Mottram et al., 2021). As a back of the envelope calculation, if the basin-wide accumulation regime shifted to one similar to what we observe in the MBS record in the 12–13th centuries (i.e., 20% less annual accumulation), this figure would decrease to around 130 $\mathrm{Gt\,yr^{-1}}$. Anomalously high snowfall has been shown

https://doi.org/10.5194/egusphere-2026-4880
Preprint. Discussion started: 18 August 2026

to result in temporary pauses in Antarctica's contribution to global sea level rise (Wang et al., 2023; Kolbe et al., 2026). The pronounced periods of low accumulation in the MBS record shows that it is equally possible that the mitigating effects of increased snowfall on sea level rise may sharply decline, if parts of the ice sheet shift to a low accumulation regime. We acknowledge that the MBS record is a site-specific reconstruction of snowfall accumulation, and our simple calculation assumes it is a basin-wide representation. However, the similarity between the 12th and 13th century low accumulation regime at MBS, and the 12th century anomalies in sea salt concentrations at Law Dome, which have been clearly related to synoptic variability in the southern Indian Ocean (Udy et al., 2022, 2024, 2026) suggests that decadal to centennial-scale natural variability is a significant feature of the atmospheric circulation (and the ensuing precipitation) in this region of East Antarctica.

MBS displays high interannual variability in snowfall accumulation during the satellite era, much of which can be explained by variability in high precipitation events at the site and in this region (Jackson et al., 2023; Turner et al., 2019; Wille et al., 2025). Our regime shift PDF analysis clearly shows different accumulation regimes are influenced by extreme years (both low and high) rather than a general increase or reduction across all years (Fig. 4). This does accord with previous studies of the satellite era at MBS. Around 50 % of annual precipitation at the MBS site comes from high and extreme precipitation events (here defined as days exceeding the 90th percentile of all precipitation days at MBS) (Jackson et al., 2023), related to large blocking highs to the east of the site, which drive strong meridional moisture transport from the southern Indian Ocean (Udy et al., 2022, 2026). In the MBS region, more than 80% of the interannual variability in total annual precipitation is explained by variability in the number of high and extreme precipitation days (Turner et al., 2019; Jackson et al., 2023). During the satellite era, the number of high precipitation days at MBS varied between 8 and 36 per year (mean = 22.3 days per year), with a very strong correlation between number of high precipitation days and annual precipitation (Jackson et al., 2023). We hypothesize that the frequency of high and extreme precipitation events is a controlling factor of centennial-scale variability in accumulation at MBS.

5.4 Optimal snowfall accumulation record derivation using site observations - recommendations from this study

Three primary sources of uncertainty exist in snowfall accumulation records: chronology error, the density adjustment, and the strain thinning adjustment. Potential MBS chronology errors are mostly well constrained through the multiple approaches to chronology development that were employed (Vance et al., 2024). In this study, we have focussed on reducing uncertainties in density and strain thinning estimates using site observations. Uncertainty in the density profile is concentrated near the surface, where density is most variable and sometimes difficult to measure accurately. Here the greatest potential bias would be overestimation of the volume, which corresponds to an underestimation of the density and therefore underestimation of the accumulation rates in the shallower parts of the core. We fit an empirical density model to the measured densities from MBS-Main to minimize error from field measurements and to get a continuous function of the density profile. In this way, we use site observations to their best advantage.

Similarly, the ApRES vertical displacement observations provide empirical data which is site specific compared to modelling thinning using the Nye (1963) model. Our comparison of both methods (Fig. S2) provides important context for our observations-heavy approach to deriving this snowfall accumulation record. Both methods assume a uniform vertical strain

https://doi.org/10.5194/egusphere-2026-4880
Preprint. Discussion started: 18 August 2026

rate with depth, but result in different long term means and trends. In comparing the two methods, the derived accumulation rates diverge significantly with age/depth (see Fig. S2). The Nye method potentially underestimates the accumulation rates at depth, resulting in what may be a spurious positive trend. In contrast, our preferred ApRES observations-based approach yields an accumulation history that does not have a long-term trend. At MBS, the Nye method results in a long term mean accumulation of 0.256 ± 0.08 m yr^{-1} ice equivalent, with a positive linear trend (2.13×10^{-5} yr^{-1} , p=0.003), roughly equal to 2 cm per millennium, compared to the ApRES approach which results in a mean accumulation of 0.276 ± 0.08 m yr^{-1} ice equivalent. The difference in long term mean accumulation between the methods is about 7%. The difference in annual accumulation rates increases with age, with the oldest layer differing by 13.7 %. A trend (whether spurious or not) must be interpreted climatologically, and can have a significant effect on both understanding past change, and the implied future trajectory of the region of the ice sheet that the ice core purports to represent. Given this, we strongly recommend future drilling campaigns should employ ApRES to measure vertical displacement, and indeed previous important drill sites could be revisited with this relatively inexpensive and easy to deploy equipment to improve their strain thinning adjustment. The implications for how we interpret the changing mass of the ice sheet through time are profound.

6 Conclusions

Here we present the new millennial-length annual snow accumulation record for the MBS ice core, East Antarctica. This record provides additional data in a particularly data-sparse region of East Antarctica, and displays a high degree of interannual, decadal and centennial-scale variability in snow accumulation, with accumulation regimes that differ significantly to other ice core records from this region of East Antarctica, such as Law Dome DSS (Roberts et al., 2015; Jong et al., 2022). Snow accumulation in the satellite era at MBS is not representative of the potential natural variability in the past millennium. This has implications for Antarctic climate studies that focus only on the satellite era when defining and projecting regional surface mass balance change. We also show that the methods used to correct for strain thinning when developing long-term accumulation rates can result in critical changes to the accumulation history at MBS, with implications more broadly for other ice core sites. We recommend a site observations based approach to deriving density and especially strain thinning adjustments, and showcase the value of ApRES measurements for this. Our study highlights the need for more high-quality long term snowfall accumulation records in data-sparse East Antarctica.

Code and data availability. Python, MATLAB and R code is available from the corresponding author on request, and will be made available upon publication. The MBS snow accumulation record, density measurements and ApRES data will be available at the Australian Antarctic Data Centre (AADC) upon publication. The MBS chronologies are available at the AADC at http://dx.doi.org/doi:10.26179/352b-6298. The MBS1998 firn density measurements are available at the AADC at http://dx.doi.org/doi:10.4225/15/5498C3D060D8E. The DSS annual snowfall accumulation data are available at the AADC at https://doi.org/10.26179/5zm0-v192. The LGB65 and 200th km accumulation data are available from the Supplement of Thomas et al. (2017).

https://doi.org/10.5194/egusphere-2026-4880
Preprint. Discussion started: 18 August 2026

The Abram SAM reconstruction is available from https://www.ncei.noaa.gov/metadata/geoportal/rest/metadata/item/noaa-recon-16197/html, the Datwyler SAM reconstruction is available at https://www.ncei.noaa.gov/access/paleo-search/study/23130, the King SAM reconstruction is available at https://zenodo.org/records/7643732, the Fogt SAM reconstruction is available at https://polarmet.osu.edu/ACD/sam/sam_recon.html, and the Marshall SAM index is available at http://www.nerc-bas.ac.uk/icd/gjma/sam.html.

Author contributions. MTN led the study, performed the data analyses and interpreted the results. MTN, TRV and PC developed the methodology. SC processed the ApRES data and assisted with interpretation. TRV, ASC and NJA contributed to field processing, density measurements and data quality control. MTN wrote the article with contributions from all authors.

Competing interests. The authors declare that they have no conflict of interest.

Acknowledgements. This project received grant funding from the Australian Government, and contributes to delivering the Australian Antarctic Science Decadal Strategy. This study was supported by the Australian Government's Antarctic Science Collaboration Initiative (ASCI000002) through funding to the Australian Antarctic Program Partnership. Logistics and analytical funding was provided by an Australian Antarctic Science grant (AAS 4414). This research was supported by the Australian Research Council Special Research Initiative, Australian Centre for Excellence in Antarctic Science (Project Number SR200100008). MTN was supported by the Australian Research Council Special Research Initiative, Australian Centre for Excellence in Antarctic Science (Project Number SR200100008), and an Australian Research Council and Tasmania Graduate Research scholarship. TRV was supported by the Australian Government's Antarctic Science Collaboration Initiative (grant no. ASCI000002) through funding to the Australian Antarctic Program Partnership. ASC received support from Polar Knowledge Canada. This study contributes to Australian Research Council Discovery Project no. DP220100606. We thank Paul Vallelonga and Jason Roberts for invaluable contributions during the field campaign.

https://doi.org/10.5194/egusphere-2026-4880
Preprint. Discussion started: 18 August 2026

References

Abram, N. J., Mulvaney, R., Vimeux, F., Phipps, S. J., Turner, J., and England, M. H.: Evolution of the Southern Annular Mode during the past millennium, Nature Climate Change, 4, 564–569, https://doi.org/10.1038/nclimate2235, 2014.

Bamber, J. L., Westaway, R. M., Marzeion, B., and Wouters, B.: The land ice contribution to sea level during the satellite era, Environmental Research Letters, 13, 063 008, https://doi.org/10.1088/1748-9326/aac2f0, 2018.

Bretherton, C. S., Widmann, M., Dymnikov, V. P., Wallace, J. M., and Bladé, I.: The Effective Number of Spatial Degrees of Freedom of a Time-Varying Field, https://journals.ametsoc.org/view/journals/clim/12/7/1520-0442_1999_012_1990_tenosd_2.0.co_2.xml, 1999.

Crockart, C. K., Vance, T. R., Fraser, A. D., Abram, N. J., Criscitiello, A. S., Curran, M. A. J., Favier, V., Gallant, A. J. E., Kittel, C., Kjær, H. A., Klekociuk, A. R., Jong, L. M., Moy, A. D., Plummer, C. T., Vallelonga, P. T., Wille, J., and Zhang, L.: El Niño–Southern Oscillation signal in a new East Antarctic ice core, Mount Brown South, Climate of the Past, 17, 1795–1818, https://doi.org/10.5194/cp-17-1795-2021, 2021.

Cuffey, K. M. and Paterson, W. S. B.: Chapter 15: Ice Core Studies, in: The Physics of Glaciers, pp. 611–674, Elsevier, 4 edn., 2010.

Dansgaard, W. and Johnsen, S. J.: A Flow Model and a Time Scale for the Ice Core from Camp Century, Greenland, Journal of Glaciology, 8, 215–223, https://doi.org/10.3189/s0022143000031208, 1969.

Dätwyler, C., Neukom, R., Abram, N. J., Gallant, A. J. E., Grosjean, M., Jacques-Coper, M., Karoly, D. J., and Villalba, R.: Teleconnection stationarity, variability and trends of the Southern Annular Mode (SAM) during the last millennium, Climate Dynamics, 51, 2321–2339, https://doi.org/10.1007/s00382-017-4015-0, 2018.

Fogt, R. L., Perlwitz, J., Monaghan, A. J., Bromwich, D. H., Jones, J. M., and Marshall, G. J.: Historical SAM Variability. Part II: Twentieth-Century Variability and Trends from Reconstructions, Observations, and the IPCC AR4 Models, https://doi.org/10.1175/2009JCLI2786.1, 2009.

Frezzotti, M., Scarchilli, C., Becagli, S., Proposito, M., and Urbini, S.: A synthesis of the Antarctic surface mass balance during the last 800 yr, The Cryosphere, 7, 303–319, https://doi.org/10.5194/tc-7-303-2013, 2013.

Gkinis, V., Jackson, S., Abram, N. J., Plummer, C., Blunier, T., Harlan, M., Kjær, H. A., Moy, A. D., Peensoo, K. M., Quistgaard, T., Svensson, A., and Vance, T. R.: An East Antarctic, sub-annual resolution water isotope record from the Mount Brown South Ice core, Scientific Data, 11, 986, https://doi.org/10.1038/s41597-024-03751-w, 2024.

Harlan, M., Kjær, H. A., de Campo, A., Svensson, A., Blunier, T., Gkinis, V., Jackson, S., Plummer, C., and Vance, T.: High resolution continuous flow analysis impurity data from the Mount Brown South ice core, East Antarctica, Earth System Science Data, 17, 6255–6271, https://doi.org/10.5194/essd-17-6255-2025, 2025.

Harlan, M. M., Fox, J., Kjær, H. A., Vance, T. R., Svensson, A., and Cook, E.: Cryptotephra in the East Antarctic Mount Brown South ice core, Climate of the Past, 22, 1057–1083, https://doi.org/10.5194/cp-22-1057-2026, 2026.

Helm, V., Humbert, A., and Miller, H.: Elevation and elevation change of Greenland and Antarctica derived from CryoSat-2, The Cryosphere, 8, 1539–1559, https://doi.org/10.5194/tc-8-1539-2014, 2014.

Herron, M. M. and Langway, C. C.: Firn Densification: An Empirical Model, Journal of Glaciology, 25, 373–385, https://doi.org/10.3189/S0022143000015239, 1980.

Jaagus, J., Sepp, M., Tamm, T., Järvet, A., and Mõisja, K.: Trends and regime shifts in climatic conditions and river runoff in Estonia during 1951–2015, Earth System Dynamics, 8, 963–976, https://doi.org/10.5194/esd-8-963-2017, 2017.

https://doi.org/10.5194/egusphere-2026-4880
Preprint. Discussion started: 18 August 2026

Jackson, S. L., Vance, T. R., Crockart, C., Moy, A., Plummer, C., and Abram, N. J.: Climatology of the Mount Brown South ice core site in East Antarctica: implications for the interpretation of a water isotope record, Climate of the Past, 19, 1653–1675, https://doi.org/10.5194/cp-19-1653-2023, 2023.

Jones, J. M., Gille, S. T., Goosse, H., Abram, N. J., Canziani, P. O., Charman, D. J., Clem, K. R., Crosta, X., de Lavergne, C., Eisenman, I., England, M. H., Fogt, R. L., Frankcombe, L. M., Marshall, G. J., Masson-Delmotte, V., Morrison, A. K., Orsi, A. J., Raphael, M. N., Renwick, J. A., Schneider, D. P., Simpkins, G. R., Steig, E. J., Stenni, B., Swingedouw, D., and Vance, T. R.: Assessing recent trends in high-latitude Southern Hemisphere surface climate, Nature Climate Change, 6, 917–926, https://doi.org/10.1038/nclimate3103, 2016.

Jong, L. M., Plummer, C. T., Roberts, J. L., Moy, A. D., Curran, M. A. J., Vance, T. R., Pedro, J. B., Long, C. A., Nation, M., Mayewski, P. A., and Van Ommen, T. D.: 2000 years of annual ice core data from Law Dome, East Antarctica, Earth System Science Data, 14, 3313–3328, https://doi.org/10.5194/essd-14-3313-2022, 2022.

King, J., Anchukaitis, K. J., Allen, K., Vance, T., and Hessl, A.: Trends and variability in the Southern Annular Mode over the Common Era, Nature Communications, 14, 2324, https://doi.org/10.1038/s41467-023-37643-1, 2023.

Kolbe, M., Torres Alavez, J. A., Mottram, R., Katurji, M., Bintanja, R., and van der Linden, E. C.: Atmospheric rivers and winter sea ice drive recent reversal in Antarctic ice mass loss, Communications Earth & Environment, 7, 255, https://doi.org/10.1038/s43247-026-03242-3, 2026.

Maclennan, M. L., Lenaerts, J. T. M., Shields, C., and Wille, J. D.: Contribution of Atmospheric Rivers to Antarctic Precipitation, Geophysical Research Letters, 49, e2022GL100 585, https://doi.org/10.1029/2022GL100585, 2022.

Marshall, G. J.: Trends in the Southern Annular Mode from Observations and Reanalyses, Journal of Climate, 16, 4134–4143, https://doi.org/10.1175/1520-0442(2003)016<4134:TITSAM>2.0.CO;2, 2003.

Matsuoka, K., Skoglund, A., Roth, G., de Pomereu, J., Griffiths, H., Headland, R., Herried, B., Katsumata, K., Le Brocq, A., Licht, K., Morgan, F., Neff, P. D., Ritz, C., Scheinert, M., Tamura, T., Van de Putte, A., van den Broeke, M., von Deschwanden, A., Deschamps-Berger, C., Van Liefferinge, B., Tronstad, S., and Melvær, Y.: Quantarctica, an integrated mapping environment for Antarctica, the Southern Ocean, and sub-Antarctic islands, Environmental Modelling & Software, 140, 105 015, https://doi.org/10.1016/j.envsoft.2021.105015, 2021.

McPhaden, M. J., Zebiak, S. E., and Glantz, M. H.: ENSO as an Integrating Concept in Earth Science, Science, 314, 1740–1745, https://doi.org/10.1126/science.1132588, 2006.

Medley, B. and Thomas, E. R.: Increased snowfall over the Antarctic Ice Sheet mitigated twentieth-century sea-level rise, Nature Climate Change, 9, 34–39, https://doi.org/10.1038/s41558-018-0356-x, 2019.

Mottram, R., Hansen, N., Kittel, C., van Wessem, J. M., Agosta, C., Amory, C., Boberg, F., van de Berg, W. J., Fettweis, X., Gossart, A., van Lipzig, N. P. M., van Meijgaard, E., Orr, A., Phillips, T., Webster, S., Simonsen, S. B., and Souverijns, N.: What is the surface mass balance of Antarctica? An intercomparison of regional climate model estimates, The Cryosphere, 15, 3751–3784, https://doi.org/10.5194/tc-15-3751-2021, 2021.

Nye, J. F.: Correction Factor for Accumulation Measured by the Thickness of the Annual Layers in an Ice Sheet, Journal of Glaciology, 4, 785–788, https://doi.org/10.3189/s0022143000028367, 1963.

Otosaka, I. N., Shepherd, A., Ivins, E. R., Schlegel, N.-J., Amory, C., van den Broeke, M. R., Horwath, M., Joughin, I., King, M. D., Krinner, G., Nowicki, S., Payne, A. J., Rignot, E., Scambos, T., Simon, K. M., Smith, B. E., Sørensen, L. S., Velicogna, I., Whitehouse, P. L., A, G., Agosta, C., Ahlstrøm, A. P., Blazquez, A., Colgan, W., Engdahl, M. E., Fettweis, X., Forsberg, R., Gallée, H., Gardner, A., Gilbert, L., Gourmelen, N., Groh, A., Gunter, B. C., Harig, C., Helm, V., Khan, S. A., Kittel, C., Konrad, H., Langen, P. L., Lecavalier, B. S., Liang, C.-

https://doi.org/10.5194/egusphere-2026-4880
Preprint. Discussion started: 18 August 2026

C., Loomis, B. D., McMillan, M., Melini, D., Mernild, S. H., Mottram, R., Mouginot, J., Nilsson, J., Noël, B., Pattle, M. E., Peltier, W. R., Pie, N., Roca, M., Sasgen, I., Save, H. V., Seo, K.-W., Scheuchl, B., Schrama, E. J. O., Schröder, L., Simonsen, S. B., Slater, T., Spada, G., Sutterley, T. C., Vishwakarma, B. D., van Wessem, J. M., Wiese, D., van der Wal, W., and Wouters, B.: Mass balance of the Greenland and Antarctic ice sheets from 1992 to 2020, Earth System Science Data, 15, 1597–1616, https://doi.org/10.5194/essd-15-1597-2023, 2023.

Rignot, E., Mouginot, J., Scheuchl, B., van den Broeke, M., van Wessem, M. J., and Morlighem, M.: Four decades of Antarctic Ice Sheet mass balance from 1979–2017, Proceedings of the National Academy of Sciences, 116, 1095–1103, https://doi.org/10.1073/pnas.1812883116, 2019.

Roberts, J., Plummer, C., Vance, T., van Ommen, T., Moy, A., Poynter, S., Treverrow, A., Curran, M., and George, S.: A 2000-year annual record of snow accumulation rates for Law Dome, East Antarctica, Climate of the Past, 11, 697–707, https://doi.org/10.5194/cp-11-697-2015, 2015.

Rodionov, S. N.: A sequential algorithm for testing climate regime shifts, Geophysical Research Letters, 31, https://doi.org/10.1029/2004GL019448, 2004.

Room, A. H., Franco-Gaviria, F., and Urrego, D. H.: rshift STARS manual: Regime shift analysis for paleoecological data, https://cran.r-project.org/web/packages/rshift/vignettes/STARSmanual.pdf, 2025.

Schröder, L., Horwath, M., Dietrich, R., Helm, V., van den Broeke, M. R., and Ligtenberg, S. R. M.: Four decades of Antarctic surface elevation changes from multi-mission satellite altimetry, The Cryosphere, 13, 427–449, https://doi.org/10.5194/tc-13-427-2019, 2019.

Shepherd, A., Ivins, E., Rignot, E., Smith, B., van den Broeke, M., Velicogna, I., Whitehouse, P., Briggs, K., Joughin, I., Krinner, G., Nowicki, S., Payne, T., Scambos, T., Schlegel, N., A, G., Agosta, C., Ahlstrøm, A., Babonis, G., Barletta, V., Blazquez, A., Bonin, J., Csatho, B., Cullather, R., Felikson, D., Fettweis, X., Forsberg, R., Gallee, H., Gardner, A., Gilbert, L., Groh, A., Gunter, B., Hanna, E., Harig, C., Helm, V., Horvath, A., Horwath, M., Khan, S., Kjeldsen, K. K., Konrad, H., Langen, P., Lecavalier, B., Loomis, B., Luthcke, S., McMillan, M., Melini, D., Mernild, S., Mohajerani, Y., Moore, P., Mouginot, J., Moyano, G., Muir, A., Nagler, T., Nield, G., Nilsson, J., Noel, B., Otosaka, I., Pattle, M. E., Peltier, W. R., Pie, N., Rietbroek, R., Rott, H., Sandberg-Sørensen, L., Sasgen, I., Save, H., Scheuchl, B., Schrama, E., Schröder, L., Seo, K.-W., Simonsen, S., Slater, T., Spada, G., Sutterley, T., Talpe, M., Tarasov, L., van de Berg, W. J., van der Wal, W., van Wessem, M., Vishwakarma, B. D., Wiese, D., Wouters, B., and The, I. t.: Mass balance of the Antarctic Ice Sheet from 1992 to 2017, Nature, 558, 219–222, https://doi.org/10.1038/s41586-018-0179-y, 2018.

Shepherd, A., Gilbert, L., Muir, A. S., Konrad, H., McMillan, M., Slater, T., Briggs, K. H., Sundal, A. V., Hogg, A. E., and Engdahl, M. E.: Trends in Antarctic Ice Sheet Elevation and Mass, Geophysical Research Letters, 46, 8174–8183, https://doi.org/10.1029/2019gl082182, 2019.

Sigl, M., McConnell, J. R., Toohey, M., Curran, M., Das, S. B., Edwards, R., Isaksson, E., Kawamura, K., Kipfstuhl, S., Krüger, K., Layman, L., Maselli, O. J., Motizuki, Y., Motoyama, H., Pasteris, D. R., and Severi, M.: Insights from Antarctica on volcanic forcing during the Common Era, Nature Climate Change, 4, 693–697, https://doi.org/10.1038/nclimate2293, 2014.

Smith, B. and Ruddell, A.: Snow accumulation in Wilhelm II Land, East Antarctica, no. 22 in Research report (Antarctic CRC), 2001.

Smith, B. T., Ommen, T. D. v., and Morgan, V. I.: Distribution of oxygen isotope ratios and snow accumulation rates in Wilhelm II Land, East Antarctica, Annals of Glaciology, 35, 107–110, https://doi.org/10.3189/172756402781816898, 2002.

Stirnimann, L., Conversi, A., and Marini, S.: Detection of regime shifts in the environment: testing "STARS" using synthetic and observed time series, ICES Journal of Marine Science, 76, 2286–2296, https://doi.org/10.1093/icesjms/fsz148, 2019.

https://doi.org/10.5194/egusphere-2026-4880
Preprint. Discussion started: 18 August 2026

Stokes, C. R., Abram, N. J., Bentley, M. J., Edwards, T. L., England, M. H., Foppert, A., Jamieson, S. S. R., Jones, R. S., King, M. A., Lenaerts, J. T. M., Medley, B., Miles, B. W. J., Paxman, G. J. G., Ritz, C., van de Flierdt, T., and Whitehouse, P. L.: Response of the East Antarctic Ice Sheet to past and future climate change, Nature, 608, 275–286, https://doi.org/10.1038/s41586-022-04946-0, 2022.

Thomas, E. R., Van Wessem, J. M., Roberts, J., Isaksson, E., Schlosser, E., Fudge, T. J., Vallelonga, P., Medley, B., Lenaerts, J., Bertler, N., Van Den Broeke, M. R., Dixon, D. A., Frezzotti, M., Stenni, B., Curran, M., and Ekaykin, A. A.: Regional Antarctic snow accumulation over the past 1000 years, Climate of the Past, 13, 1491–1513, https://doi.org/10.5194/cp-13-1491-2017, 2017.

Thomas, E. R., Vladimirova, D. O., Tetzner, D. R., Emanuelsson, B. D., Chellman, N., Dixon, D. A., Goosse, H., Grieman, M. M., King, A. C. F., Sigl, M., Udy, D. G., Vance, T. R., Winski, D. A., Winton, V. H. L., Bertler, N. A. N., Hori, A., Laluraj, C. M., McConnell, J. R., Motizuki, Y., Takahashi, K., Motoyama, H., Nakai, Y., Schwanck, F., Simões, J. C., Lindau, F. G. L., Severi, M., Traversi, R., Wauthy, S., Xiao, C., Yang, J., Mosely-Thompson, E., Khodzher, T. V., Golobokova, L. P., and Ekaykin, A. A.: Ice core chemistry database: an Antarctic compilation of sodium and sulfate records spanning the past 2000 years, Earth System Science Data, 15, 2517–2532, https://doi.org/10.5194/essd-15-2517-2023, 2023.

Turner, J., Phillips, T., Thamban, M., Rahaman, W., Marshall, G. J., Wille, J. D., Favier, V., Winton, V. H. L., Thomas, E., Wang, Z., Van Den Broeke, M., Hosking, J. S., and Lachlan-Cope, T.: The Dominant Role of Extreme Precipitation Events in Antarctic Snowfall Variability, Geophysical Research Letters, 46, 3502–3511, https://doi.org/10.1029/2018gl081517, 2019.

Udy, D., Jackson, S., Vance, T. R., Pohl, B., Kiem, A. S., Holbrook, N. J., Plummer, C., Wille, J. D., Favier, V., Crockart, C., Harlan, M., Abram, N., Long, C. A., Nation, M., Christoffersen, P., and King, M.: Weather Regimes Preclude the Observation of a Southern Annular Mode Signal in Two Coastal East Antarctic Ice Cores, Journal of Geophysical Research: Atmospheres, 131, e2025JD045 013, https://doi.org/10.1029/2025JD045013, _eprint: https://agupubs.onlinelibrary.wiley.com/doi/pdf/10.1029/2025JD045013, 2026.

Udy, D. G., Vance, T. R., Kiem, A. S., Holbrook, N. J., and Curran, M. A. J.: Links between Large-Scale Modes of Climate Variability and Synoptic Weather Patterns in the Southern Indian Ocean, Journal of Climate, 34, 883–899, https://doi.org/10.1175/jcli-d-20-0297.1, 2021.

Udy, D. G., Vance, T. R., Kiem, A. S., and Holbrook, N. J.: A synoptic bridge linking sea salt aerosol concentrations in East Antarctic snowfall to Australian rainfall, Communications Earth & Environment, 3, 175, https://doi.org/10.1038/s43247-022-00502-w, 2022.

Udy, D. G., Vance, T. R., Kiem, A. S., Holbrook, N. J., and Abram, N.: Australia's 2019/20 Black Summer fire weather exceptionally rare over the last 2000 years, Communications Earth & Environment, 5, 317, https://doi.org/10.1038/s43247-024-01470-z, 2024.

Van Ommen, T. D., Morgan, V. I., Jacka, T. H., Woon, S., and Elcheikh, A.: Near-surface temperatures in the Dome Summit South (Law Dome, East Antarctica) borehole, Annals of Glaciology, 29, 141–144, https://doi.org/10.3189/172756499781821382, 1999.

Vance, T. R., Ommen, T. D. v., Curran, M. A. J., Plummer, C. T., and Moy, A. D.: A Millennial Proxy Record of ENSO and Eastern Australian Rainfall from the Law Dome Ice Core, East Antarctica, https://doi.org/10.1175/JCLI-D-12-00003.1, 2013.

Vance, T. R., Roberts, J. L., Plummer, C. T., Kiem, A. S., and van Ommen, T. D.: Interdecadal Pacific variability and eastern Australian megadroughts over the last millennium, Geophysical Research Letters, 42, 129–137, https://doi.org/10.1002/2014GL062447, 2015.

Vance, T. R., Roberts, J. L., Moy, A. D., Curran, M. A. J., Tozer, C. R., Gallant, A. J. E., Abram, N. J., Van Ommen, T. D., Young, D. A., Grima, C., Blankenship, D. D., and Siegert, M. J.: Optimal site selection for a high-resolution ice core record in East Antarctica, Climate of the Past, 12, 595–610, https://doi.org/10.5194/cp-12-595-2016, 2016.

Vance, T. R., Kiem, A. S., Jong, L. M., Roberts, J. L., Plummer, C. T., Moy, A. D., Curran, M. A. J., and van Ommen, T. D.: Pacific decadal variability over the last 2000 years and implications for climatic risk, Communications Earth & Environment, 3, 33, https://doi.org/10.1038/s43247-022-00359-z, 2022.

https://doi.org/10.5194/egusphere-2026-4880
Preprint. Discussion started: 18 August 2026

Vance, T. R., Abram, N. J., Criscitiello, A. S., Crockart, C. K., Decampo, A., Favier, V., Gkinis, V., Harlan, M., Jackson, S. L., Kjær, H. A., Long, C. A., Nation, M. K., Plummer, C. T., Segato, D., Spolaor, A., and Vallelonga, P. T.: An annually resolved chronology for the Mount Brown South ice cores, East Antarctica, Climate of the Past, 20, 969–990, https://doi.org/10.5194/cp-20-969-2024, 2024.

Vaňková, I., Nicholls, K. W., Corr, H. F. J., Makinson, K., and Brennan, P. V.: Observations of Tidal Melt and Vertical Strain at the Filchner-Ronne Ice Shelf, Antarctica, Journal of Geophysical Research: Earth Surface, 125, e2019JF005 280, https://doi.org/10.1029/2019JF005280, _eprint: https://agupubs.onlinelibrary.wiley.com/doi/pdf/10.1029/2019JF005280, 2020.

Wang, Y., Wu, Q., Zhang, X., and Zhai, Z.: Record-breaking Antarctic snowfall in 2022 delays global sea level rise, Science Bulletin, 68, 3154–3157, https://doi.org/10.1016/j.scib.2023.08.055, 2023.

Wille, J., Alexander, S., Amory, C., Baiman, R., Barthélemy, L., Bergstrom, D., Berne, A., Binder, H., Blanchet, J., Bozkurt, D., Bracegirdle, T., Casado, M., Choi, T., Clem, K., Codron, F., Datta, R., Battista, S., Favier, V., Francis, D., and Zou, X.: The Extraordinary March 2022 East Antarctica "Heat" Wave. Part II: Impacts on the Antarctic Ice Sheet, Journal of Climate, 37, 779–799, https://doi.org/10.1175/JCLI-D-23-0176.1, 2024.

Wille, J. D., Favier, V., Gorodetskaya, I. V., Agosta, C., Baiman, R., Barrett, J. E., Barthelemy, L., Boza, B., Bozkurt, D., Casado, M., Chyhareva, A., Clem, K. R., Codron, F., Datta, R. T., Durán-Alarcón, C., Francis, D., Hoffman, A. O., Kolbe, M., Krakovska, S., Linscott, G., Maclennan, M. L., Mattingly, K. S., Mu, Y., Pohl, B., Santos, C. L.-D., Shields, C. A., Toker, E., Winters, A. C., Yin, Z., Zou, X., Zhang, C., and Zhang, Z.: Atmospheric rivers in Antarctica, Nature Reviews Earth & Environment, 6, 178–192, https://doi.org/10.1038/s43017-024-00638-7, 2025.

Winstrup, M., Vallelonga, P., Kjær, H. A., Fudge, T. J., Lee, J. E., Riis, M. H., Edwards, R., Bertler, N. A. N., Blunier, T., Brook, E. J., Buizert, C., Ciobanu, G., Conway, H., Dahl-Jensen, D., Ellis, A., Emanuelsson, B. D., Hindmarsh, R. C. A., Keller, E. D., Kurbatov, A. V., Mayewski, P. A., Neff, P. D., Pyne, R. L., Simonsen, M. F., Svensson, A., Tuohy, A., Waddington, E. D., and Wheatley, S.: A 2700-year annual timescale and accumulation history for an ice core from Roosevelt Island, West Antarctica, Climate of the Past, 15, 751–779, https://doi.org/10.5194/cp-15-751-2019, 2019.